

Parity Violation and Chiral Oscillation of Cosmological Relic Neutrinos

Shao-Feng Ge^{1,2,*} and Pedro Pasquini^{1,†}

¹*Tsung-Dao Lee Institute, Shanghai Jiao Tong University, Shanghai 200240, China*

²*School of Physics and Astronomy, Shanghai Jiao Tong University,
Shanghai Key Laboratory for Particle Physics and Cosmology, Shanghai 200240, China*

The conventional derivation of neutrino oscillation treats neutrino mass eigenstate as plane wave with an overall evolution phase. Nevertheless, due to the intrinsic parity-violating nature of weak interactions, only the left-chiral neutrino can be produced as initial condition. On the other hand, the neutrino mass term connects the left-chiral component to the right-chiral one and unavoidably leads to generation of the later through oscillation. This chiral oscillation has significant consequences on the detection of the cosmological relic neutrinos. The event rate is reduced by a factor of 2 than the conventional prediction.

Introduction – The neutrino oscillation [1–3] was established by the atmospheric [4] and solar [5, 6] neutrino experiments. It indicates that the active neutrinos are massive, rather than massless particles as assumed in the Standard Model (SM) of particle physics [7]. This is the first new physics beyond the SM.

Although neutrino is a fermion that is described by spinor [8], the conventional derivation [9] simply takes each neutrino mass eigenstate ν_i as a plane wave, $\nu_i(x) = e^{-ip \cdot x} \nu_i$, where p and x are the 4-momentum and coordinates, to describe the neutrino oscillation, completely neglecting the chiral nature of neutrinos. In this formalism, the neutrino oscillation happens among different flavors. Nevertheless, this approach is far from being enough.

The oscillation effect is intimately related to the tiny neutrino masses. To make the effect of the tiny mass differences explicit, the neutrino propagation and oscillation should happen over large enough distance. Although we infer nonzero neutrino masses from neutrino oscillations, it is difficult to make the chiral properties of neutrinos manifest due to the smallness of neutrino masses. Neutrinos can be effectively described by the two-component theory [10]. Practically, the tiny neutrino masses also make it very difficult to distinguish Dirac and Majorana neutrinos [11].

The incorporation of the spinor nature of neutrinos in the oscillation leads naturally to what is called the chiral oscillation [12–15] and also gives rise to the interesting phenomena of neutrino-antineutrino oscillation for Majorana fields [1, 16–20]. On top of that, another type of phenomena can appear in the relativistic theory of fermion propagators, such as helicity flip and the coupling with magnetic fields [21, 22].

To make the spinor nature of neutrino oscillation explicit, we need low energy neutrino flux. The cosmological relic neutrinos from the early Universe is a perfect test ground for this purpose. Their energy is typically of the order of meV as predicted by the Cosmological Standard Model [23]. In this paper, we evaluate the phenomenological consequences of spinor oscillation on the cosmic neutrino background (CνB) for both Dirac and Majorana types.

Chiral Oscillation – Two things need to be incorporated into the description of neutrino oscillation. First, the neutrino interactions in the SM violate parity [24]. In both the neutral and charged current interactions, only left-chiral neutrino appears while the right-chiral one is completely absent. It is then not reasonable to take the neutrino mass eigenstate as a whole particle by treating its evolution with just an overall phase $e^{-ip \cdot x}$ without considering its spinor nature. Instead, only the left-chiral neutrino can be created at the production point.

During the propagation, the left-chiral neutrino oscillates to its right-chiral counterpart due to the connection established by the mass term. A derivation with operator projections can be found in [13–15]. Here we provide a more intuitive derivation. For a neutrino with fixed momentum

$$\nu(t, \mathbf{x}) = \nu(t) e^{i\mathbf{p} \cdot \mathbf{x}} = \begin{pmatrix} \varphi(t) \\ \chi(t) \end{pmatrix} e^{i\mathbf{p} \cdot \mathbf{x}}, \quad (1)$$

we parametrize the time dependence as $\varphi(t)$ and $\chi(t)$. The Dirac equation written explicitly in terms of chiral components looks like,

$$\begin{pmatrix} m & -i\partial_t + \boldsymbol{\sigma} \cdot \mathbf{p} \\ -i\partial_t - \boldsymbol{\sigma} \cdot \mathbf{p} & m \end{pmatrix} \begin{pmatrix} \varphi(t) \\ \chi(t) \end{pmatrix} = 0. \quad (2)$$

Without mass, the left- and right-chiral components disentangle from each other. In other words, the mass makes it possible to express $\chi(t)$ in terms of $\varphi(t)$,

$$\chi(t) = \frac{1}{m} [i\partial_t + \mathbf{p} \cdot \boldsymbol{\sigma}] \varphi(t). \quad (3)$$

Only one of $\chi(t)$ and $\varphi(t)$ is independent. The solution can be generally parametrized as

$$\varphi(t) = C_1 \cos(Et) + C_2 i \sin(Et), \quad (4)$$

where E is the neutrino energy while C_1 and C_2 denote two spinors. Substituting $\varphi(t)$ into Eq. (3), the corresponding $\chi(t)$ can be obtained,

$$\chi(t) = \frac{1}{m} [(\mathbf{p} \cdot \boldsymbol{\sigma} C_1 - C_2 E) \cos(Et) + i(-EC_1 + \mathbf{p} \cdot \boldsymbol{\sigma} C_2) \sin(Et)]. \quad (5)$$

The initial condition requires $\chi(t=0) = 0$, establishing correlation among the two spinors, $C_2 = (\mathbf{p} \cdot \boldsymbol{\sigma}/E)C_1$. For the production of a left-chiral neutrino, the spinor C_1 is exactly the initial $\varphi(0)$. A similar calculation can be performed for an initial right-chiral antineutrino. The oscillating neutrino then becomes

$$\nu(t) = \left[\cos(Et) - \frac{i}{E} (2c\mathbf{p} \cdot \mathbf{S} + m\gamma_0) \sin(Et) \right] \nu_c, \quad (6)$$

where $c = \mp$ for left- and right-chiral components $\nu_c = \nu_{L,R}$, respectively, for generality. As we can see, switching the chirality in Eq. (2) changes the sign in front of the momentum.

The spin operator is defined as, $\mathbf{S} \equiv \frac{1}{2} \text{diag}\{\boldsymbol{\sigma}, \boldsymbol{\sigma}\}$. Consequently, $2\mathbf{p} \cdot \mathbf{S}\nu^h = |\mathbf{p}|h\nu^h$ extracts the helicity eigenvalue $h \equiv \pm$. Note that γ_0 does not change spinor helicity. Although the neutrino spinor oscillates among different chiralities, its helicity is conserved. A more explicit form is

$$\nu(t) = \left\{ \left[c_E - ich \frac{|\mathbf{p}|}{E} s_E \right] - \frac{m}{E} s_E \gamma_0 \right\} \nu_c, \quad (7)$$

where we have defined $[c_E, s_E] \equiv [\cos(Et), \sin(Et)]$ for simplicity. The first term of Eq. (7) conserves chirality while the second changes it. In the massless limit, $m \ll E$, the evolution reduces to just a chirality-conserving overall phase, $\nu_c^h(t) = e^{-ichEt} \nu_c^h$. On the other hand, the non-relativistic limit gives a maximal oscillation between the left- and right-chiral components, $\nu(t) = c_E \nu_L - s_E \nu_R$, where $\nu_R \equiv \gamma_0 \nu_L$. Note that this oscillation happens even with only one flavor of neutrino,

$$P_{\nu_L \rightarrow \nu_L} = |c_L|^2 = \cos^2(Et) + \frac{|\mathbf{p}|^2}{E^2} \sin^2(Et), \quad (8a)$$

$$P_{\nu_L \rightarrow \nu_R} = |c_R|^2 = \frac{m^2}{E^2} \sin^2(Et). \quad (8b)$$

In the SM, this Majorana spinor can be composed as, $\nu_M = \nu_L + \mathcal{C}\bar{\nu}_L^T$. The Dirac equation of Majorana fields, $i\cancel{\partial}\nu_L = m\mathcal{C}\bar{\nu}_L^T$ [8] and equivalently $i\cancel{\partial}\mathcal{C}\bar{\nu}_L^T = m\nu_L$ can group into the same form as Eq. (2). And the initial left-chiral Majorana neutrino in the relativistic limit would unavoidably have both chiralities in the non-relativistic limit [25]. The chiral oscillation Eq. (6) applies for both Dirac and Majorana neutrinos. With these taken into consideration, the Majorana condition, $\nu_M^c(t) = \nu_M(t)$, holds for chiral oscillation at an arbitrary time. Valuable discussions can be found in [26–29].

Chiral Evolution of Cosmic Neutrinos – Since the chiral oscillation is induced by the nonzero mass, its effect is most significant at the nonrelativistic limit. However, the neutrino masses are very tiny, being at the sub-eV scale. It is very difficult to find low-energy neutrino fluxes to test the chiral oscillation with parity violation.

Fortunately, the cosmic relic neutrinos created at the early stage of the expanding Universe have cooled down to low enough energy and hence can serve as a perfect place for testing the chiral oscillation.

The evolution of the neutrino states can be described by the Boltzmann equation [30],

$$\mathbb{L}(\rho) \equiv (\partial_t - H\mathbf{p} \cdot \nabla_{\mathbf{p}}) \rho = -i[\mathbb{H}, \rho], \quad (9)$$

where H is the Hubble constant and \mathbb{H} is the Hamiltonian,

$$\mathbb{H} = \mathbf{p} \cdot (\gamma_0 \boldsymbol{\gamma}) + m\gamma_0 = \begin{pmatrix} h|\mathbf{p}| & m \\ m & -h|\mathbf{p}| \end{pmatrix}, \quad (10)$$

in the chiral basis. The left-hand side of the Boltzmann equation is the Liouville operator \mathbb{L} which incorporates the Hubble expansion. On the other hand, the right-hand side is not from the collision that a Boltzmann equation usually describes but from the chiral oscillation. With chiral decomposition, the density matrix also becomes a 2×2 matrix,

$$\rho \equiv \begin{pmatrix} \rho_{LL} & \rho_{LR} \\ \rho_{LR}^* & \rho_{RR} \end{pmatrix}, \quad (11)$$

where ρ_{LL} and ρ_{RR} stand for the fraction of the left- and right-chiral components, respectively.

To make it more explicit, we may regroup the density matrix elements, $\rho_{\pm} \equiv \rho_{LL} \pm \rho_{RR}$, $\rho_R \equiv \mathbb{R}(\rho_{LR})$ and $\rho_I \equiv \mathbb{I}(\rho_{LR})$. The total probability ρ_+ is conserved, $\mathbb{L}[\rho_+] = 0$, since its contribution to the ρ matrix commutes with the Hamiltonian. The remaining ρ_- , ρ_R , and ρ_I are related to each other.

Since the Hubble constant is typically smaller than the neutrino mass, the solution can be obtained by series expansion of $\epsilon \equiv H/m$. The leading order result is,

$$\rho_- = 1 - \frac{2m^2}{E^2} \sin^2(Et), \quad (12a)$$

$$\rho_R + i\rho_I = \frac{hm|\mathbf{p}|}{E^2} \sin^2(Et) + i\frac{m}{E} \sin(2Et). \quad (12b)$$

The next order expansion solution is $\lesssim 1\%$ in the limit $|\mathbf{p}_0| \ll m$ at the current time.

For the typical $m = \mathcal{O}(10^{-3} \sim 10^{-2})$ eV neutrinos, the chiral oscillation is fast enough, in comparison to the big time difference between neutrino decoupling to now, $t_0 - t_d \sim 6 \times 10^{38} \text{MeV}^{-1}$. The averaged result becomes,

$$\langle \rho_- \rangle = 1 - \frac{m^2}{E^2}, \quad \langle \rho_R \rangle = \frac{hm|\mathbf{p}|}{E^2}, \quad \langle \rho_I \rangle = 0. \quad (13)$$

For neutrinos today with very small redshift, its momentum is much smaller than its mass ($|\mathbf{p}_0| \ll m$) or equivalently $E \approx m$, leading to $\rho_- = 0$. Hence, the relic neutrinos today have equal contributions from the left- and right-chiral components, $\rho_{LL} = \rho_{RR} = 1/2$, even

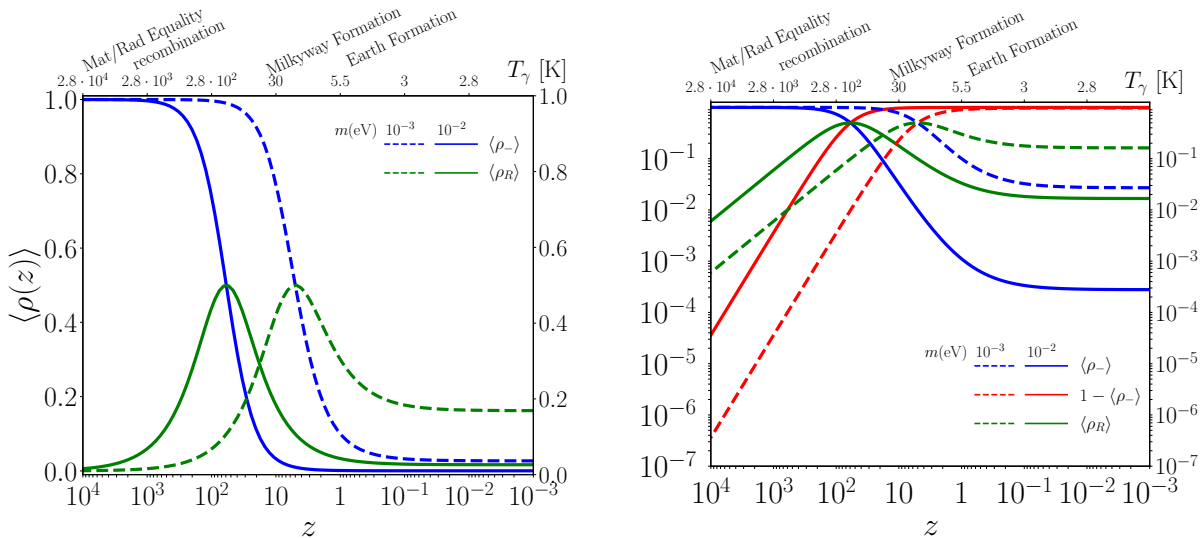


FIG. 1. Evolution of the chiral density matrix elements $\langle \rho_{-} \rangle$ (blue) or $1 - \langle \rho_{-} \rangle$ (red), and $\rho_R = \mathbb{R}[c_L c_R^*]$ (green) as functions of the redshift z for $m = 10^{-2}$ eV (solid) and $m = 10^{-3}$ eV (dashed) with $|\mathbf{p}_d| = 1$ MeV. The redshift at neutrino decoupling is taken to be $z_d \sim 6 \times 10^9$.

though at the beginning there was only left-chiral component. Since ρ_I averages out, we only need to consider $\langle \rho_{-} \rangle$ and $\langle \rho_R \rangle$ in the following discussions.

The results are shown in Fig. 1 as a function of the redshift z or CMB temperature T_γ for $m = 10^{-2}$ eV (solid line) and $m = 10^{-3}$ eV (dashed line), together with a typical decoupling momentum $|\mathbf{p}_d| = 1$ MeV which corresponds to $|\mathbf{p}_0| \sim 1.66 \times 10^{-4}$ eV at the present time. The neutrino decoupling happened at redshift $z_d \sim 6 \times 10^9$. The current redshift is $z_0 = 0$ and temperature around 2.75 K $\sim 2.4 \times 10^{-4}$ eV. Due to the Universe expansion, the particle momentum gets redshifted as $|\mathbf{p}(z)| = (1+z)|\mathbf{p}_0|$. The solutions Eq. (12) are actually functions of the redshift z . The behavior of the curves of $\langle \rho_{-} \rangle$ and $\langle \rho_R \rangle$ can be understood analytically,

$$1 - \langle \rho_{-} \rangle \approx \frac{\hat{\rho}_0^2}{(1+z)^2 + \hat{\rho}_0^2}, \quad \langle \rho_R \rangle \approx \frac{\hat{\rho}_0(1+z)}{(1+z)^2 + \hat{\rho}_0^2}, \quad (14)$$

where $\hat{\rho}_0 \equiv m/|\mathbf{p}_0| \sim 6 \times 10^4 (\frac{m}{\text{eV}})$. Notice that $\langle \rho_R \rangle$ has a maximum at $z_{\text{peak}} \equiv \hat{\rho}_0 - 1$, where $\langle \rho_R \rangle = \langle \rho_{-} \rangle = 1/2$ that also appears as a crossing point between the $1 - \langle \rho_{-} \rangle$ and $\langle \rho_R \rangle$ curves. Since the redshift has to be positive, this can only occur if $\hat{\rho}_0 \geq 1$ or $m \geq |\mathbf{p}_0| \sim 1.66 \times 10^{-4}$ eV. For comparison, we show in Fig. 1 a solid line for $m = 10^{-2}$ eV and a dashed line for $m = 10^{-3}$ eV. Consequently, there is a shift almost one order of magnitude in the position of the peak between these two cases. The solid line peaks at $z_{\text{peak}} = 599$ while the dashed one at $z_{\text{peak}} = 59$.

We may further explore the behaviors at the large red-

shift $z \gg \hat{\rho}_0$,

$$1 - \langle \rho_{-} \rangle \approx \frac{\hat{\rho}_0^2}{z^2} = \frac{m^2}{|\mathbf{p}_0|^2 z^2}, \quad \langle \rho_R \rangle \approx \frac{\hat{\rho}_0}{z} = \frac{m}{|\mathbf{p}_0| z}. \quad (15)$$

To make the scaling behaviors more explicit, we show log-scale plots in the right plot of Fig. 1. The slope of the red $1 - \langle \rho_{-} \rangle$ curves for large z is -2 while the one for the green $\langle \rho_R \rangle$ curve is -1 . Since it is a log-log plot, the intersection of the curves with the y-axis is determined by the relative size of m and $|\mathbf{p}_0|$. The m^2 dependence induces two orders of magnitude difference between the two intersections, $1 - \langle \rho_{-} \rangle(z = 10^4) \sim 3.6 \times 10^{-5}$ for $m = 10^{-2}$ eV and 3.6×10^{-7} for $m = 10^{-3}$ eV on the y-axis. On the other hand, the green curve has only one order of magnitude difference, $\langle \rho_R \rangle(z = 10^4) \sim 6 \times 10^{-3}$ for $m = 10^{-3}$ eV and 6×10^{-2} for $m = 10^{-2}$ eV due to the linear m dependence.

At small redshift, the curves have asymptotic values

$$\langle \rho_{-} \rangle(z \rightarrow 0) \approx \frac{\hat{\rho}_0^2}{(1 + \hat{\rho}_0^2)} \approx 2.8 \times (10^{-4}, 10^{-2}), \quad (16a)$$

$$\langle \rho_R \rangle(z \rightarrow 0) \approx \frac{\hat{\rho}_0}{(1 + \hat{\rho}_0^2)} \approx 1.7 \times (10^{-2}, 10^{-1}), \quad (16b)$$

for $m = (10^{-2}, 10^{-3})$ eV, respectively. This explains the flat behavior of the curves in the small z region. For $m = |\mathbf{p}_0| \sim 1.66 \times 10^{-4}$ eV, the asymptotic values are $\langle \rho_R \rangle(z \rightarrow 0) = 1 - \langle \rho_{-} \rangle(z \rightarrow 0) = 1/2$. Any value between $[0, 1/2]$ can be obtained if $m < |\mathbf{p}_0|$ and the vanishing value 0 occurs for $m \rightarrow 0$, where no transition between the left- and right-chiral components can occur.

Detection of Cosmic Neutrinos – The chiral oscillation has important consequences on the chiral composition of

relic neutrinos. To make a uniform description for the Dirac and Majorana cases, we denote the four chiral and helicity components of neutrino/antineutrino as ν_c^\pm , with $c = L, R$ representing the chirality and \pm the helicity, respectively. Although all these four states can in principle be created even with just left-chiral current interactions, the right-chiral neutrino (ν_L^+) and left-chiral antineutrino (ν_R^-) are highly suppressed by a factor of $m^2/E^2 < 10^{-12}$ due to the high temperature and hence large neutrino momentum at the decoupling time and therefore can be safely ignored [25]. Nevertheless, these missing states (ν_L^+ and ν_R^-) will become populated through chiral oscillation as elaborated above. This can change the event number of cosmic neutrino background detection at the PTOLEMY experiment [31].

At production, neutrinos are in thermal equilibrium and hence follow the Fermi-Dirac distribution with number densities $n(\nu_L^-) = n(\nu_R^+) = n(z_d)$ while $n(\nu_L^+) = n(\nu_R^-) = 0$. In the presence of chiral oscillation, the original number densities $n(\nu_L^-)$ and $n(\nu_R^+)$ of neutrino and antineutrino, respectively, splits into left/right-chiral components. To be more specific, the averaged solution Eq. (13) indicates that the neutrino number density is redistributed as,

$$n(\nu_L^-) = n_0 \left(1 - \frac{m^2}{2E^2}\right), \quad \text{and} \quad n(\nu_R^-) = n_0 \frac{m^2}{2E^2}. \quad (17)$$

Similar things happen for the anti-neutrino mode. The full results are summarized in the left half of Tab. I. Since the same chiral oscillation properties apply for both Dirac and Majorana neutrinos, the neutrino number densities in Tab. I also apply universally.

For comparison, we also show the case without considering chiral oscillation. After decoupling, the number densities are then fixed and decreases with a^3 if we do not take into account neutrino chiral oscillation. From the neutrino decoupling ($z_d \sim 6 \times 10^9$) to the present time ($z = 0$), the temperature drops from 1 MeV to 0.168 meV, resulting in $n_0 \equiv n(z = 0) = 56 \text{ cm}^{-3}$ [25]. Without considering chiral oscillation, there is no need to distinguish different chiralities, but only $n(\nu^\pm)$. The results have been summarized in the right half of Tab. I.

Since relic neutrinos are nonrelativistic, the most feasible way of detecting them is through neutrino capture on tritium (T) [31, 32]. The squared matrix element is,

$$|\mathcal{M}|^2 = \langle {}^3\text{He} e^- | \mathcal{L}_{\text{int}} | T \nu \rangle \langle \nu T | \mathcal{L}_{\text{int}} | {}^3\text{He} e^- \rangle. \quad (18)$$

The quantity $|\nu\rangle\langle\nu|$ encodes the density matrix in Eq. (11). Another way of seeing this quantity is through the evolved spinor in Eq. (6). In the usual charged-current interaction, $\mathcal{L}_{\text{int}} \equiv \frac{g}{\sqrt{2}} W_\mu^- \bar{\ell} \gamma^\mu P_L \nu$, the second part gives an extra detection possibility only for Majorana neutrinos.

Due to parity violation, only the left-chiral neutrino and the right-chiral anti-neutrino appear in the interaction. In addition, energy conservation selects neutron in

| | w/ Chiral Osc. | | | w/o Chiral Osc. | | |
|--------------|----------------------------|---|------------|----------------------------|----------------------------|-------|
| | $z = z_{\text{fo}}$ | $z = 0$ | | $z = z_{\text{fo}}$ | $z = 0$ | |
| $n(\nu_L^-)$ | $n_0(1 + z_{\text{fo}})^3$ | $n_0 \left(1 - \frac{m^2}{2E^2}\right)$ | $n(\nu^-)$ | $n_0(1 + z_{\text{fo}})^3$ | n_0 | |
| $n(\nu_R^-)$ | 0 | $n_0 \frac{m^2}{2E^2}$ | | | | |
| $n(\nu_L^+)$ | 0 | $n_0 \frac{m^2}{2E^2}$ | | $n(\nu^+)$ | $n_0(1 + z_{\text{fo}})^3$ | n_0 |
| $n(\nu_R^+)$ | $n_0(1 + z_{\text{fo}})^3$ | $n_0 \left(1 - \frac{m^2}{2E^2}\right)$ | | | | |

TABLE I. The neutrino number densities at neutrino decoupling ($z_d \approx 6 \times 10^9$) and today ($z = 0$) for all the four different chirality and helicity components ($\nu_L^-, \nu_R^-, \nu_L^+$, and ν_R^+). The number density $n_0 = 56 \text{ cm}^{-3}$ is obtained according to the Fermi-Dirac distribution for the neutrino temperature $T_\nu \approx 0.168 \text{ meV}$ [25].

the tritium nuclei as the initial and proton as the final states. Then, charge conservation selects electron in the final state. For relativistic neutrinos, only the left-chiral neutrino can be detected. At low energy, only neutrino can contribute for the Dirac case while the two helicity states have equal contributions for the Majorana case,

$$N_{\nu_D} = \bar{\sigma} N_T \left(1 + \frac{|\mathbf{p}|}{E}\right) n(\nu_L^-), \quad (19a)$$

$$N_{\nu_M} = \bar{\sigma} N_T \left[\left(1 + \frac{|\mathbf{p}|}{E}\right) n(\nu_L^-) + \left(1 - \frac{|\mathbf{p}|}{E}\right) n(\nu_R^+) \right], \quad (19b)$$

where N_T is the number of targets in the detector. The factors $1 \pm |\mathbf{p}|/E$ are associated with helicities, $h = \mp$, respectively, and the cross section $\bar{\sigma}$ can be found in [25]. Without chiral oscillation, $n(\nu^-) = n(\nu^+) = n_0$, leading to the ratio between the Majorana/Dirac event rates as: $N_{\nu_M}/N_{\nu_D} \approx 2$. In the presence of chiral oscillation, the chiral components experience frequent oscillation to and from each other. The averaged number densities have been summarized in Tab. I. In the nonrelativistic limit, $|\mathbf{p}| \rightarrow 0$, $n(\nu_L^-) = n(\nu_R^+) = n(\nu_L^+) = n(\nu_R^-) = n_0/2$. The expected $C\nu B$ event rates are reduced to half of the conventional prediction without chiral oscillation.

Conclusions – We explore the phenomenological consequences of parity violation and chirality mixture of the neutrino mass term on neutrino oscillation for both Dirac and Majorana neutrino. Even with only one flavor, the left- and right-chiral components can already oscillate to and from each other. This has a significant consequence on the detection of the cosmic neutrino background. Although helicity is conserved in chiral oscillation, the neutrino chirality changes and the neutrino number density equality splits into the two chiral components. This reduces the event rate of the $C\nu B$ detection by a factor of 2. Once knowing whether neutrinos are Dirac or Majorana fermions, we can test chiral oscillation with $C\nu B$ detection.

Notes Added – During the finalization of this paper, we notice a similar work [33] about the phenomenological consequences of chiral oscillation on the cosmological relic neutrinos.

Acknowledgement – SFG is grateful to the Double First Class start-up fund (WF220442604) provided by Tsung-Dao Lee Institute and Shanghai Jiao Tong University. SFG would like to thank Yu-Feng Li for useful discussions.

* gesf@sjtu.edu.cn

† ppasquini@sjtu.edu.cn

- [1] B. Pontecorvo, “*Mesonium and anti-mesonium*,” Sov. Phys. JETP **6**, 429 (1957).
- [2] Z. Maki, M. Nakagawa and S. Sakata, “*Remarks on the unified model of elementary particles*,” Prog. Theor. Phys. **28**, 870 (1962).
- [3] B. Pontecorvo, “*Neutrino Experiments and the Problem of Conservation of Leptonic Charge*,” Sov. Phys. JETP **26**, 984 (1968) [Zh. Eksp. Teor. Fiz. **53**, 1717 (1967)].
- [4] Y. Fukuda *et al.* [Super-Kamiokande], “*Evidence for oscillation of atmospheric neutrinos*,” Phys. Rev. Lett. **81**, 1562-1567 (1998) [hep-ex/9807003 [hep-ex]].
- [5] J. N. Bahcall, “*Solar neutrinos. I: Theoretical*,” Phys. Rev. Lett. **12**, 300-302 (1964); R. Davis, “*Solar neutrinos. II: Experimental*,” Phys. Rev. Lett. **12**, 303-305 (1964).
- [6] Q. R. Ahmad *et al.* [SNO], “*Measurement of the rate of $\nu_e + d \rightarrow p + p + e^-$ interactions produced by 8B solar neutrinos at the Sudbury Neutrino Observatory*,” Phys. Rev. Lett. **87**, 071301 (2001) [nucl-ex/0106015 [nucl-ex]].
- [7] S. Weinberg, “*A Model of Leptons*,” Phys. Rev. Lett. **19**, 1264-1266 (1967); S. L. Glashow, “*Partial Symmetries of Weak Interactions*,” Nucl. Phys. **22**, 579-588 (1961); A. Salam, “*Weak and Electromagnetic Interactions*”, in Svartholm N., Elementary Particle Theory, Stockholm, Almquist and Wiksell, 1968.
- [8] C. Giunti and C. W. Kim, “*Fundamentals of Neutrino Physics and Astrophysics*,”
- [9] S. M. Bilenky and B. Pontecorvo, “*Lepton Mixing and Neutrino Oscillations*,” Phys. Rept. **41**, 225 (1978); B. Kayser, “*On the Quantum Mechanics of Neutrino Oscillation*,” Phys. Rev. D **24**, 110 (1981).
- [10] T. D. Lee and C. N. Yang, “*Parity Nonconservation and a Two Component Theory of the Neutrino*,” Phys. Rev. **105**, 1671-1675 (1957).
- [11] B. Kayser, “*Majorana Neutrinos and their Electromagnetic Properties*,” Phys. Rev. D **26**, 1662 (1982).
- [12] S. De Leo and P. Rotelli, “*Neutrino chiral oscillations*,” Int. J. Theor. Phys. **37**, 2193-2206 (1998) [arXiv:hep-ph/9605255 [hep-ph]].
- [13] A. E. Bernardini and S. D. Leo, “*Flavor and chiral oscillations with Dirac wave packets*,” Phys. Rev. D **71**, 076008 (2005) [hep-ph/0504239].
- [14] A. E. Bernardini, “*Chiral oscillations in terms of the zitterbewegung effect*,” Eur. Phys. J. C **50**, 673-678 (2007) [arXiv:hep-th/0701091 [hep-ph]].
- [15] A. E. Bernardini, M. M. Guzzo and C. C. Nishi, “*Quantum flavor oscillations extended to the Dirac theory*,” Fortsch. Phys. **59**, 372 (2011) [arXiv:1004.0734 [hep-ph]].
- [16] J. Schechter and J. W. F. Valle, “*Neutrino Oscillation Thought Experiment*,” Phys. Rev. D **23**, 1666 (1981).
- [17] L. F. Li and F. Wilczek, “*Physical Processes Involving Majorana Neutrinos*,” Phys. Rev. D **25**, 143 (1982).
- [18] P. Langacker and J. Wang, “*Neutrino anti-neutrino transitions*,” Phys. Rev. D **58**, 093004 (1998) [hep-ph/9802383 [hep-ph]].
- [19] A. de Gouvea, B. Kayser and R. N. Mohapatra, “*Manifest CP Violation from Majorana Phases*,” Phys. Rev. D **67**, 053004 (2003) [hep-ph/0211394].
- [20] Z. z. Xing, “*Properties of CP Violation in Neutrino-Antineutrino Oscillations*,” Phys. Rev. D **87**, no. 5, 053019 (2013) [arXiv:1301.7654 [hep-ph]]; Z. z. Xing and Y. L. Zhou, “*Majorana CP-violating phases in neutrino-antineutrino oscillations and other lepton-number-violating processes*,” Phys. Rev. D **88**, 033002 (2013) [arXiv:1305.5718 [hep-ph]].
- [21] A. Popov and A. Studenikin, “*Neutrino eigenstates and flavour, spin and spin-flavour oscillations in a constant magnetic field*,” Eur. Phys. J. C **79**, no.2, 144 (2019) [arXiv:1902.08195 [hep-ph]].
- [22] P. Pustoshny, V. Shakhov and A. Studenikin, “*Neutrino spin and spin-flavour oscillations in matter currents and magnetic fields*,” [arXiv:2001.03691 [hep-ph]].
- [23] A. D. Dolgov, “*Neutrinos in cosmology*,” Phys. Rept. **370**, 333-535 (2002) [hep-ph/0202122 [hep-ph]].
- [24] T. D. Lee and C. N. Yang, “*Question of Parity Conservation in Weak Interactions*,” Phys. Rev. **104**, 254-258 (1956).
- [25] A. J. Long, C. Lunardini and E. Sabancilar, “*Detecting non-relativistic cosmic neutrinos by capture on tritium: phenomenology and physics potential*,” JCAP **08**, 038 (2014) [arXiv:1405.7654 [hep-ph]].
- [26] M. Dvornikov, “*Field theory description of neutrino oscillations*,” Neutrinos: Properties, Sources and Detection, ed. by J.P.Greene, Nova Science Publishers, New York, 2011, p. 23-90 [arXiv:1011.4300 [hep-ph]].
- [27] S. Esposito and N. Tancredi, “*Pontecorvo neutrino - anti-neutrino oscillations: Theory and experimental limits*,” Mod. Phys. Lett. A **12**, 1829-1838 (1997) [arXiv:hep-ph/9705351 [hep-ph]].
- [28] S. Esposito, “*Flavor conserving oscillations of Dirac-Majorana neutrinos*,” Int. J. Mod. Phys. A **13**, 5023-5036 (1998) [arXiv:hep-ph/9802336 [hep-ph]].
- [29] M. Fukugita and T. Yanagida, “*Physics of neutrinos and applications to astrophysics*”.
- [30] P. F. de Salas and S. Pastor, “*Relic neutrino decoupling with flavour oscillations revisited*,” JCAP **07**, 051 (2016) [arXiv:1606.06986 [hep-ph]].
- [31] M. G. Betti *et al.* [PTOLEMY], “*Neutrino physics with the PTOLEMY project: active neutrino properties and the light sterile case*,” JCAP **07**, 047 (2019) [arXiv:1902.05508 [astro-ph.CO]].
- [32] S. Weinberg, “*Universal Neutrino Degeneracy*,” Phys. Rev. **128**, 1457-1473 (1962)
- [33] V. A. S. V. Bittencourt, A. E. Bernardini and M. Blason, “*Chiral oscillations in the non-relativistic regime*,” [arXiv:2009.00084 [hep-ph]].